A 500 kV Nanosecond Pulse Generator Based on an Off-the-Shelf Solid-State Opening Switch

Mawuena Rémi Degnon, Anton Gusev, Antoine Silvestre de Ferron, Laurent Pecastaing, Arthur Piaser, Frédéric Bayol, Sébastien Boisne, Bucur Mircea Novac

A 500 kV Nanosecond Pulse Generator Based on an Off-the-Shelf Solid-State Opening Switch

Mawuena R. Degnon, Anton I. Gusev, *Member, IEEE*, Antoine Silvestre de Ferron, Laurent Pecastaing, *Senior Member, IEEE*, Arthur Piaser, Frédéric Bayol, Sébastien Boisne, and Bucur M. Novac, *Senior Member, IEEE*

***Abstract*—This article investigates the use of Off-The-Shelf (OTS) diodes as opening switches in a 500 kV nanosecond pulsed power generator. A 40 J test bench based on a saturable pulse transformer and on a primary thyratron switch is designed to evaluate the performance of the OTS diodes in comparison with standard Semiconductor Opening Switch (SOS) diodes. A distinguishing feature of the proposed circuit is the adjustability of the output pulse energy, which is achieved using flat hysteresis loop magnetic cores and variable reset magnetic field. The study confirms the operation of OTS diodes as an opening switch, although highlighting differences in the reverse current conduction that affect the generated voltage pulse characteristics. Based on the successful operation of the OTS diodes, a 500 kV pulsed power Generator using an OTS Solid-State Opening Switch (GO-SSOS) was developed. The GO-SSOS provides output voltages of 100 – 500 kV across a 50 Ω – 1 kΩ resistive load, with a pulse width of about 100 ns and a rise time of less than 40 ns. The generator achieves a peak power of 335 MW and demonstrates an overall energy efficiency in the range of 30% to 70% depending on the load. Operation at a pulse repetition rate of 60 Hz is presented, showing a good reproducibility of the pulses with an amplitude and duration deviation of about 2% and 10%, respectively. No degradation of the OTS diodes has been observed after the tests (more than 1000 pulses). As an example of the possible applications of the GO-SSOS, corona discharge in the air was performed, also proving the stability of all the systems under conditions of strong electromagnetic interference.**

***Index Terms*—Nanosecond pulse generator, off-the-shelf diode, pulsed power systems, saturable pulse transformer, semiconductor diodes, Semiconductor Opening Switch (SOS).**

I. Introduction

INTEREST in the field of pulsed power is constantly growing, mainly due to its wide range of potential applications across various fields. While historically concentrated within the military sector [1], recent decades have witnessed a notable expansion into civilian domains. The versatility of pulsed power systems is highlighted by their utility in numerous applications including gas and liquid treatment [2], exploration of electrophysical properties of semiconductors and dielectrics [3], electron beams and radiation techniques for sterilization and food processing [4], [5], as well as the electropermeabilization of biological cells using pulsed electric field techniques [6]. This expanding scope of application has made pulsed power generators increasingly attractive to industry. In particular, the use of electrical energy instead of chemical processes in sterilization technology [7] motivates this work.

In industrial settings, pulsed power generators have to comply with stringent requirements, including high reliability, long lifetime, maintenance-free operation, high pulse repetition frequency, and adjustable output parameters, to suit specific needs. Semiconductor devices perfectly match these criteria. However, when it comes to generating repetitive high-voltage pulses of several hundred kilovolts, only a few solid-state solutions are capable of doing so. Among these are the Semiconductor Opening Switch (SOS) [8], solid-state Marx [9], and magnetic switch-based [10] pulsed power generators. SOS generators stand out, in particular, for their ability to produce nanosecond megavolt voltage impulses, generate gigawatt peak powers, and operate at a pulse repetition frequency (PRF) of several kilohertz [11]. These generators use inductive energy storage, which has a higher energy density compared to capacitive energy storage systems according to [12].

The heart of SOS generators is the SOS diode, which consists of a stack of silicon diodes designed to interrupt high currents with densities superior to 1 kA/cm² in nanosecond duration [11]. Compared to standard rectifying diodes, SOS diodes have a specific "$p^+ - p - n - n^+$" doping profile, characterized by an extended $p-$region of about 200 µm [13]. The number of p-n junctions in an SOS stack determines the rated voltage of the switch, hence it must be increased to block high voltages. Moreover, the energy capacity of SOS diodes can be enhanced by parallel connections of the diodes to avoid thermal breakdown, which can occur at current densities close to 100 kA/cm² [11], [14]. Additionally, appropriate diode cooling enables operation at high PRF, increasing the average power, which is crucial for industrial applications.

Although SOS generators are an ideal candidate for repetitive nanosecond high-voltage generation, the lack of SOS diode manufacturers prevents their widespread use. Therefore, the present study investigates the feasibility of using off-the-

Manuscript submitted in March 2024.

This work was supported in part by the French "Investissements d'Avenir" Program within the Framework of the Energy and Environment Solutions (E2S) Université de Pau et des Pays de l'Adour (UPPA) Project [Solid-State Pulsed Power (S2P2) and Pulsed Power Applications (PULPA) Chairs] managed by the Agence Nationale de la Recherche (ANR) under Grant ANR-16-IDEX-0002 and in part by ITOPP ALCEN.

Mawuena R. Degnon is with the Universite de Pau et des Pays de l'Adour, E2S UPPA, SIAME, Pau, France, and also with ITOPP ALCEN, 46500 Thégra, France (e-mail: mdegnon@univ-pau.fr).

Anton I. Gusev, Antoine Silvestre de Ferron, and Laurent Pecastaing are with the Universite de Pau et des Pays de l'Adour, E2S UPPA, SIAME, Pau, France, (e-mail: anton.gusev@univ-pau.fr).

Arthur Piaser, Frédéric Bayol, and Sébastien Boisne are with ITOPP ALCEN, Thégra, France (e-mail: FBayol@itopp-alcen.com).

Bucur M. Novac is with the Wolfson School of Mechanical, Electrical and Manufacturing Engineering, Loughborough University, LE11 3TU Leicestershire, Loughborough, U.K., and also with the Universite de Pau et des Pays de l'Adour, E2S UPPA, SIAME, Pau, France, (e-mail: b.m.novac@lboro.ac.uk).

shelf (OTS) diodes as an opening switch in pulsed power systems. Our previous study [15] has revealed the potential of OTS diodes to operate in the opening switch mode at switching energies below 10 J. Diodes with blocking voltages of a few kilovolts, maximum forward surge currents of up to a few kiloamperes, and recovery times reaching several microseconds were of interest. In this work, avalanche, fast recovery, rectifier, and transient voltage suppressor (TVS) diodes were tested. The results indicate that the most promising OTS diodes are TVS and fast recovery diodes. The OTS-100 (100 kV max) diode assembled using fast recovery diodes has succeeded in generating a voltage pulse of amplitude reaching 90 kV with a rise time of 20-35 ns and a Full Width at Half Maximum (FWHM) within 60-105 ns.

Building on this work, the present study focuses on switching energies higher than 10 J, with the aim of generating voltage pulses of up to 500 kV at a PRF of several tens of hertz, using the OTS fast recovery diodes. To this end, a 40 J test bench is developed.

This article is organized as follows. An overview of the experimental setup and the design of the components is presented in Section II. The comparative analysis of the OTS and SOS diodes across various operation points is given in Section III. The 500 kV pulsed power generator prototype based on the OTS diode is presented in the same section. Finally, a summary is provided in Section IV.

II. Circuit Principle and Generator Design

A. Circuit Layout and Operation Principle

The high-voltage part of the test bench is illustrated in Fig.1. It includes a step-up saturable pulse transformer SPT, which transfers energy from the primary capacitor C1 into the secondary capacitor C2 in resonance mode, providing the forward and reverse pumping of the opening switch diode SOS. When the diode switches, interrupting the current, the energy is delivered to the resistive load R_L, forming the output voltage pulse.

To be energy-efficient, the circuit uses a single magnetic element – SPT. This approach, however, requires a primary switch S1, capable of withstanding high voltage, high current, and high rate of rise of current (dI/dt). Although there are solid-state solutions of S1 [16], [17], a thyratron is used in this work for simplicity. The dump resistor R1 and protective diode D1 are installed to prevent the reverse voltage across the thyratron in the event of a circuit failure or mismatched load. In order to ensure efficient transmission of the energy from the primary to the secondary capacitor, the magnetic bias circuit consisting of the current source I_s, choke CK, and bias winding w_b, is used to magnetize the SPT core before each pulse. A detailed analysis of the magnetic bias circuit utility is available in [18].

The circuit operates as follows. Capacitor C1 is charged using the 9 kW capacitor charger CCR50KV-4J (V_{source}). When S1 is triggered, the stored energy in C1 undergoes discharge through the primary winding w_1 of the SPT and resonantly charges C2. The charging current of C2 flows through the SOS, providing the forward pumping current. The

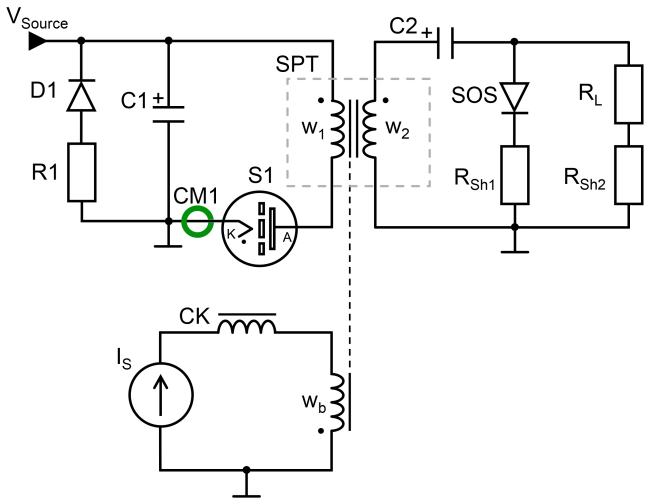

Fig. 1. Circuit diagram of the high-voltage part of the opening switch test bench with an energy stored in C1 of up to 40 J. Description of the components is provided in the text.

transformer is designed to saturate at the maximum voltage on C2, when the forward current through the SOS diode is zero. At this time, the forward pumping stage is over.

Capacitor C2 then discharges through the SPT secondary winding w_2 and SOS diode, storing energy in inductive storage, which consists of the saturated inductance of the secondary winding and the parasitic inductance of the circuit. During this process, the reverse pumping of the SOS diode takes place. Subsequently, the diode cuts off the reverse current – ideally at its maximum – when all energy has been transferred to the inductive storage. The current is therefore transmitted to the load, resulting in a nanosecond high-voltage pulse with an amplitude V_{R_L} highly dependent on the load.

B. Description of the Main Components

1) Capacitors and Primary Switch

Ceramic high-voltage capacitors TDK UHV-9A (2 nF, 40 kV) are used to assemble C1 (50 in parallel) and C2 (10 in series, 3 in parallel). Their capacitances (C1 = 100 nF and C2 = 620 pF) are matched according to the SPT transformation ratio to maximize the energy transfer efficiency (w_1 = 1 turn and w_2 = 12 turns).

In addition to C1 voltage, the amplitude and dI/dt of the current flowing through the SPT primary winding are essential parameters in the design of the primary switch S1. These current parameters result from a typical SOS forward pumping time of 500 ns. The inductance of the primary side can be calculated as 0.5 µH by applying the Thomson formula expressing the period T of an oscillating LC circuit:

$$T = 2\pi\sqrt{LC}\ , \qquad (1)$$

where L is the inductance of the circuit and C is the capacitance. The inductance calculation allows estimating the current amplitude (8 kA) and dI/dt (50 kA/µs) that must be handled by the primary switch when C1 is charged to 25 kV. The precise calculation of the inductance is given in Section III.

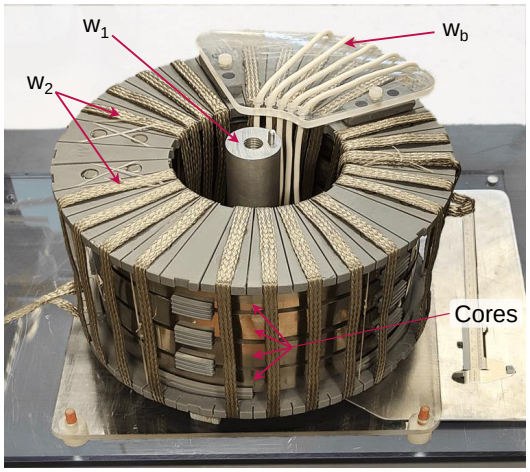

Fig. 2. Picture of the SPT showing the four nanocrystalline cores with primary, secondary, and bias windings.

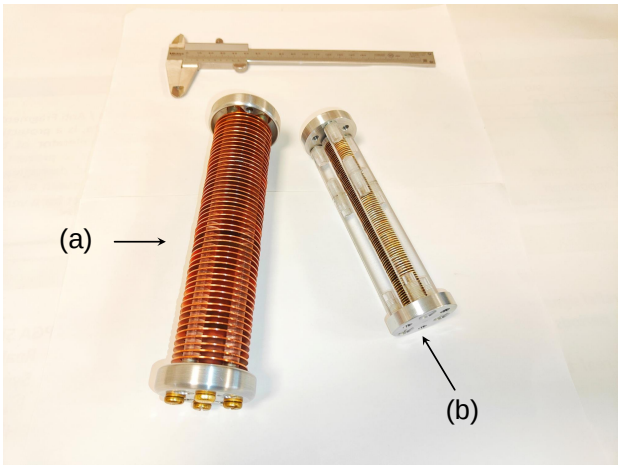

Fig. 3. Picture of the opening switches showing (a) an SOS-180-4 (265 kV max) and (b) an OTS-150 (150 kV max).

The CX1174 thyratron, rated for 40 kV and 40 kA, meets the requirements of the S1 primary switch. It features two grids that are triggered by a double voltage pulse, to optimize triggering characteristics and switching performance as recommended in [19]. The triggering pulses, along with the reservoir and cathode heating currents, are supplied by an in-house assembled driving system. This system primarily relies on a standard North Star TT-G1/G2 driver [20], which generates the double trigger pulse. The driving system also includes two power supplies providing the heating currents, which are monitored by Hall effect current sensors. The thyratron driver is controlled by an Atmega328p microcontroller-based system (Arduino Uno R3), which communicates with the peripherals via a fiber-optic interface.

2) *Saturable Pulse Transformer*

Considering an optimal overvoltage coefficient of the opening switch of about 2 [11], the maximum voltage on C2 is assumed to be 250 kV to reach a load voltage of 500 kV. With a primary voltage V_{C1} of 25 kV, a transformation ratio n of 12 is determined with some margins, taking into account losses in the primary switch and SPT. The primary winding consists of a single turn to minimize its inductance and energy transfer time. The secondary winding is divided into two parallel sections of 12 turns each, in order to reduce its inductance, mostly in the saturated state. More details on the SPT design technique can be found in [18].

The cross-sectional area of the SPT magnetic core is derived from the voltage-time product [21]:

$$2\Delta B \times S_C \times N = V_{max} \times T_{sat} \ , \qquad (2)$$

where ΔB is the magnetic induction swing, S_c is the effective material cross-section, N is the number of turns of the secondary winding, V_{max} is the peak voltage across C2, and T_{sat} is the saturation time, which corresponds to the forward pumping duration of about 500 ns. Using the Finemet FT-3L nanocrystalline material of saturation induction Bs = 1.2 T, the required S_c is found to be approximately 22 cm². The geometric cross-section of 30 cm² is determined, considering the packing factor k = 0.73 due to interlaminar insulation of the tape wound core. Four toroidal cores of 256 x 165.2 x 25 mm^3 have been used instead of a bulky single core, to improve cooling. The SPT with its primary, secondary, and bias windings is depicted in Fig. 2.

The winding supports and insulating spacers are 3D printed using liquid resin. The SPT is designed to operate in transformer oil. Taking into account the volume dielectric strength of 36 kV/mm of the transformer oil (Diala S4), the minimum distance between the winding and the core was chosen to be 13 mm in all directions, ensuring a safety margin of 3 times. The spacers of 4 mm thickness between two consecutive cores allow better cooling of the cores by oil circulation.

The primary winding consists of an aluminum rod of 40 mm diameter and 180 mm height. The secondary winding is made of a 10 mm width braiding cable housed in dedicated notches to ensure insulation between turns. Additional grooves on the winding support increase the electrical path between two consecutive turns. The magnetic bias winding of 5 turns is used to reset the core before each pulse.

3) *Opening Switch*

Two opening switches have been investigated in the framework of this research: (i) the SOS-180-4 (265 kV max) diode which serves as a reference and (ii) the OTS-150 (150 kV max) diode which is assembled from off-the-shelf rectifier diodes used in [15]. Fig. 3 shows the assembled diodes, and their typical parameters are listed in Table I.

4) *Diagnostics*

A Pearson current monitor Model 101 (CM1) is used to measure the current through the primary switch S1 (Fig. 1). Two in-house made current shunts R_{Sh1} = 0.15 Ω and R_{Sh2} = 0.5 Ω are connected in series to the SOS and the load, respectively, to measure their current independently. The North Star PVM100 and the homemade 600 kV Capacitive Divider (CD) described in [22] are employed to validate the load voltage obtained

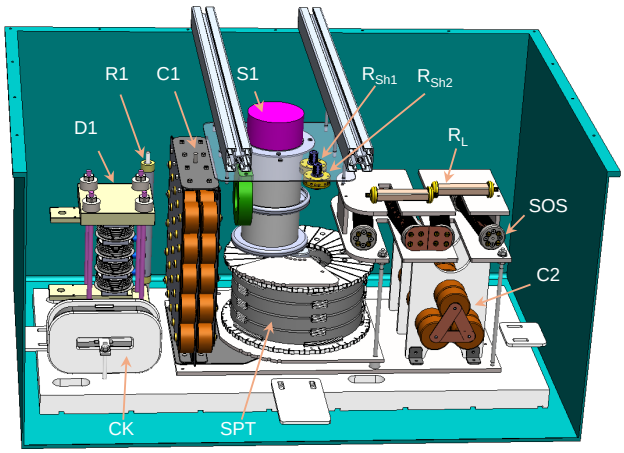

Fig. 4. Overview of the high-voltage part of the experimental arrangement.

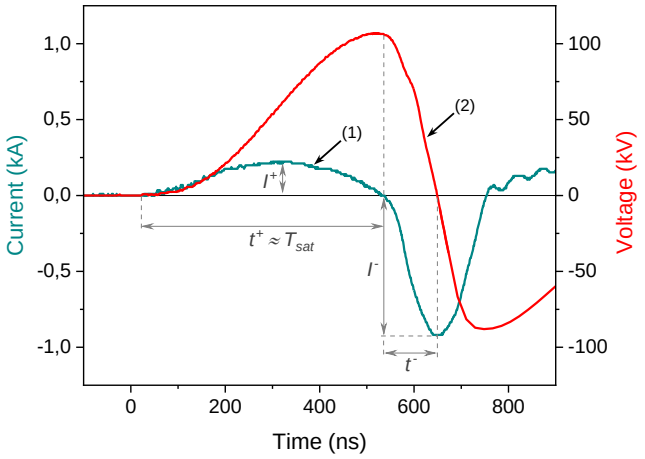

Fig. 5. Waveforms of the current through the secondary winding (1) and the voltage across C2 (2) during the short circuit experiment, when C1 is charged to 10 kV (E_{C1} = 5 J).

while using R_{Sh2}. The CD features an equivalent capacitance of 12.4 pF, an attenuation of -82 dB, and a bandwidth ranging from 8 Hz to 55 MHz. The primary voltage on C1 is measured using a North Star PVM12 probe. The voltage and current signals are captured using the real-time digital oscilloscopes: Tektronix TDS7704B (7 GHz, 20 Gs/s) and MSO56 (2 GHz, 6.25 Gs/s). The signals are attenuated using 4 GHz RF-LAMBDA attenuators.

The experimental setup is depicted in Fig. 4, providing an overview of the arrangement. All the components are inserted inside the tank of dimensions 104 x 71 x 55 cm^3 (length x width x height). The tank housing all the components is filled with 300 liters of Diala S4 transformer oil. The entire system has a total mass of less than 350 kg. For practical reasons, this prototype intentionally features a large volume of the tank. Therefore, the size and weight can be decreased for an industrial system. The parameters of the main components are described in Table I.

III. Results and Discussion

A. Transformer Characterization

To characterize the SPT, a short circuit experiment was performed. In this experiment, the secondary winding was connected in series with C2 and R_{Sh1}. The current through the SPT secondary winding and voltage across C2 is presented in Fig. 5 when C1 is charged to 10 kV. From these waveforms, it can be seen that the core saturation occurs when C2 voltage reaches its maximum, thanks to the magnetic field applied by the bias circuit (Fig. 1). The saturation time T_{sat} of about 512 ns is measured at the point where the slope of the current curve changes (Fig. 5).

The short circuit experiment can be used to determine the actual inductance of the circuit, which is defined by the transformer winding, circuit components, and connections. Using (3), these inductances are found to be approximately 0.53 µH and 88 µH for the primary and secondary sides, respectively.

$$L_w = \frac{(T_{sat})^2}{\pi^2 \times C_{eq}} \ , \tag{3}$$

where C_{eq} represents the capacitance of the equivalent circuit referring to the primary ($C_{eq} \approx \frac{C1}{2}$) or secondary ($C_{eq} \approx \frac{C2}{2}$) side.

The secondary winding inductance drops to 7 µH when the pulse transformer saturates. Moreover, the saturated transformer decouples the primary and secondary circuits, and, as a result, C_{eq} is equal to C2. Consequently, the amplitude and duration of the reverse current are respectively 4.2 times higher and 2.4 times shorter than the forward current parameters (Fig. 5).

TABLE I
Parameters of the Circuit Components

Component	Type	Parameters
Capacitor C1	TDK-UHV-9A	*100 nF, 40 kV*
Capacitor C2		*620 pF, 400 kV*
Switch S1	Thyratron CX1174	*40 kV, 40 kA, 150 kA/µs*
Transformer SPT	Finemet FT-3L	*$n = 12$, $Bs = 1.2$ T, $S_c = 32$ cm²*
Opening switch SOS	SOS-180-4	*265 kV max, 4 kA reverse current*
	OTS-150	*150 kV max*
Load R_L	TVO	*From 50 Ω to 1 kΩ*

B. Comparison of SOS and OTS

The investigation of the diodes was performed using the circuit presented in Fig. 1. In the low-resistance load experiment, C1 was charged to 25 kV, which corresponds to 31.3 J stored in the primary energy storage. The resistive load was measured to be 49 Ω. The opening switches consisted of a single OTS-150 and a single SOS diode stack. The number of diodes in the SOS stack was arranged in order to have the same blocking voltage of about 150 kV in this experiment. The two diodes were tested in almost identical conditions provided by the circuit when the energy is transferred from C1 to C2.

The obtained results are presented in Fig. 6. In both cases, the charging voltage of C2 is 242 kV. This voltage is determined through the integration of the discharge current of C2 ($I_{C2} = I_{R_{Sh1}} + I_{R_{Sh2}}$). For both diodes, the forward pumping current amplitude I^+ and duration t^+ are about 500 A and 440 ns, respectively. The on-state resistances of the diodes, calculated at the maximum amplitude I^+, are comparable, i.e. 1.2 Ω for the SOS diodes versus 2.8 Ω for the OTS-150.

Despite having similar forward pumping conditions, the two diodes react differently to the reverse current. Whereas the SOS diode allows the reverse current to flow up to its maximum of 2.2 kA, the OTS diode interrupts it earlier, when the reverse current reaches 0.9 kA. With the SOS diode, the voltage pulse across the load comes mainly from the inductive energy storage, since the current is interrupted close to its peak at the reverse pumping time t^- of 71 ns. At this moment, about 93% of the energy stored in C2 ($E_{C2} = 18.2\ J$) is transferred to the intermediate inductive storage L_w of 7 µH. Conversely, the early interruption of the current by the OTS leads to hybrid energy storage, since the energy stored in the capacitor C2 is not fully transferred into inductive storage. Indeed, at the moment of current interruption by the OTS-150, only 16% of the capacitive energy has been transferred to the inductance.

This early interruption of the current by the OTS diodes was first observed in [15] when the OTS diode was pumped in similar conditions in a 10 J test bench. Even though the OTS diodes' typical recovery time falls within the range of 0.6 µs to 0.9 µs, according to the data sheet, their operation in the test bench exhibits nanosecond reverse current conduction times as short as 26 ns, when the forward current duration is about 440 ns. This short reverse conduction of the OTS diode may be attributed to the lifetime controlling processes of carriers in silicon power devices, involving methods such as diffusion of impurities like gold and platinum, or the creation of traps in the silicon lattice by high-energy particles [23]. However, since the structure and doping profile of the diodes are not disclosed, further research is required for a thorough understanding of their switching mechanism.

After the OTS diode has interrupted the current, the residual energy in capacitor C2 simply discharges into the load. The RC time constant calculated for the 49 Ω load corresponds to 31 ns. The combination of the inductive and capacitive energy discharges in the load forms the output pulse using the OTS diode. The main parameters of current and voltage amplitudes and durations are summarized in Table II.

In the high-resistance load experiment, the primary energy stored was increased to 36.5 J, and the load of about 1 kΩ was installed to reach voltages of up to 500 kV. As a single SOS-180-4 diode had proven its ability to withstand pulse voltages of amplitude up to 265 kV in a previous study, the SOS diode assembly consisted of two SOS-180-4 connected in series, while the OTS was assembled using four OTS-150 diodes.

The results are presented in Fig. 7 and Table III. In this configuration, the inductive energy amounts to 90% with the SOS diode and to 16% with the OTS diode, out of the total energy of 22 J stored in C2. The peak cut-off current I^- is 2.4 kA for the SOS diode and the current through the 960 Ω load is 530 A. For the OTS, these parameters are respectively

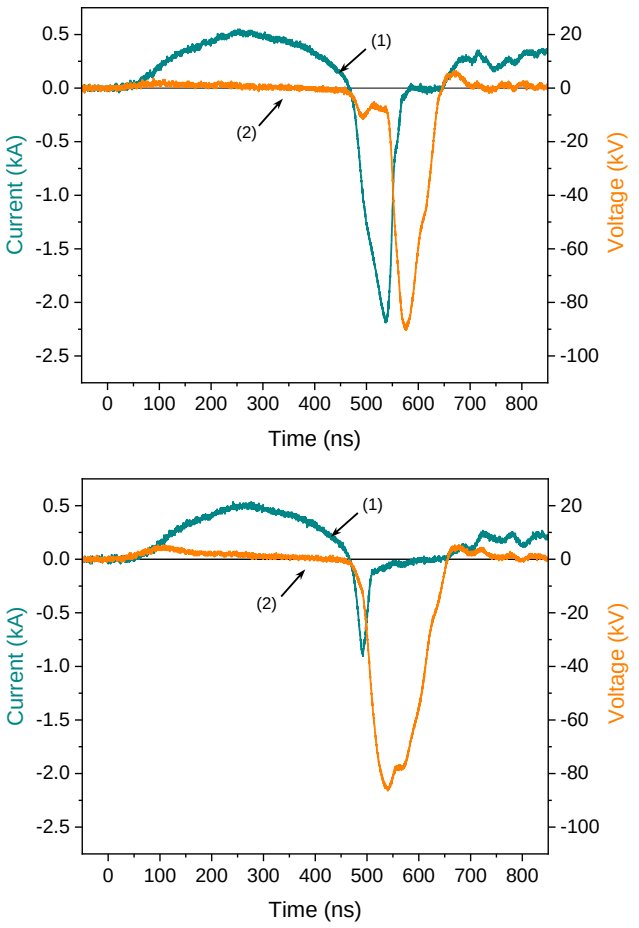

Fig. 6. Waveforms of the current through the diode (1) and voltage at the 49 Ω load (2) for (a) SOS diode stack (150 kV max) and (b) OTS-150 (150 kV max), with a primary energy E_{C1} of 31.3 J.

TABLE II
DIODE CURRENT AND LOAD VOLTAGE PARAMETERS AT 50 Ω

	DBV* (kV)	I^+ (kA)	I^- (kA)	t^+ (ns)	t^- (ns)	V_{R_L} (kV)	T_r** (ns)	FWHM (ns)
SOS	150	0.52	2.2	440	71	90	26	63
OTS	150	0.49	0.9	440	26	85	38	105

* DBV – Diode Blocking Voltage.

** From 10% to 90% of V_{R_L}.

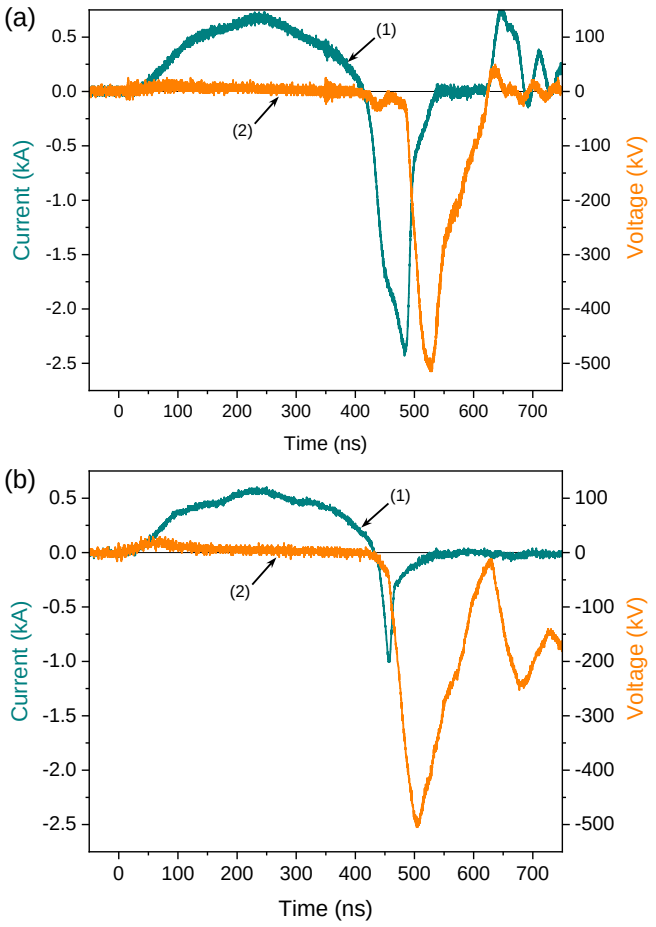

Fig. 7. Waveforms of the current through the diode (1) and voltage across the load (2) for (a) two SOS-180-4 in series (530 kV max) with R_L = 960 Ω, and (b) four OTS-150 in series (600 kV max) with R_L = 940 Ω, at a primary energy E_{C1} = 36.5 J.

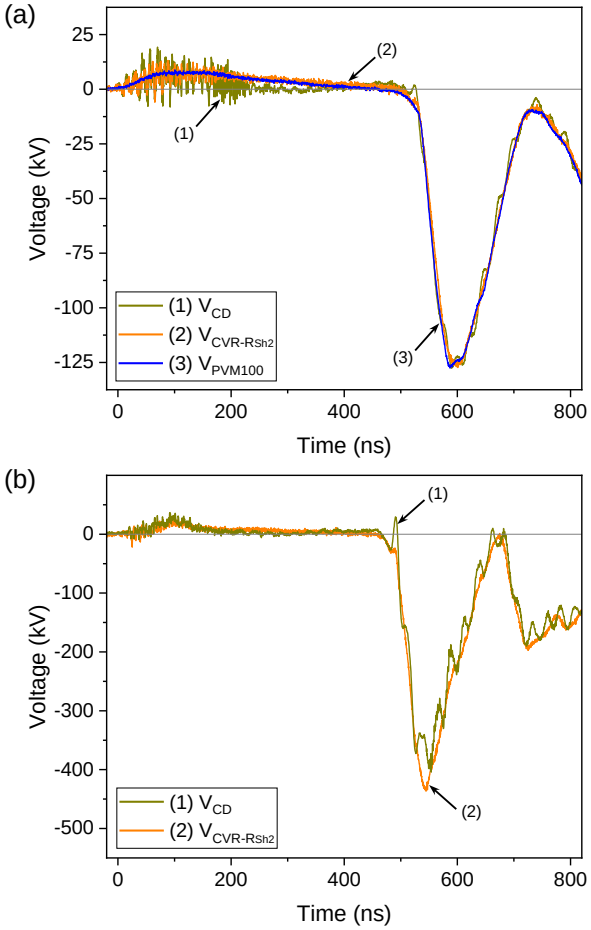

Fig. 8. Load voltage waveforms obtained at 1 kΩ load, using the capacitive divider CD (1), the current viewing resistor R_{Sh2} (2), and the PVM100 probe (3) for (a) low voltage (E_{C1} = 4 J) and (b) high voltage (E_{C1} = 31.3 J).

TABLE III
DIODE CURRENT AND LOAD VOLTAGE PARAMETERS AT 1 KΩ

	DBV (kV)	I^+ (kA)	I^- (kA)	t^+ (ns)	t^- (ns)	V_{R_L} (kV)	T_r (ns)	FWHM (ns)
SOS	530	0.7	2.4	400	70	509	26	60
OTS	600	0.6	1	425	25	498	38	84

1 kA and 530 A when the load is 940 Ω. Thus, the targeted output voltage of 500 kV was successfully reached using both opening switches, even though with the OTS diode, the circuit does not operate as an ideal inductive storage system.

Unlike the operation with a low resistive load, at a high load, the voltage pulse obtained with the OTS diode breaks down into a main pulse (from 430 ns to 630 ns in Fig. 7 (b)) followed by oscillations whose intensity decreases with time. In our opinion, this is due to the oscillation of the residual energy in C2 after the diode interrupts the current, because of the parasitic capacitance which is estimated to be about 50 pF through SPICE simulation. However, the energy of the main pulse obtained with the OTS diode (16 J) is greater than that with the SOS diode (12 J). The reason is likely the lower switching losses of the OTS diodes since the reverse current is interrupted earlier.

As mentioned in Section II, additional capacitive probes (PVM100 and CD) are employed to confirm the accuracy of the voltage measurement method using the R_{Sh2} current viewing resistor and the load value. Fig. 8 (a) shows the voltage pulse measured using the three probes. This comparison at the same time serves for the calibration of the CD using the PVM100 probe, which is rated for a maximum of 150 kV. For higher voltages, the measurement is performed using CD and R_{Sh2} (Fig. 8 (b)). Notably, the voltage amplitude deviation of less than 10% and the time difference of less than 1% confirm the accuracy of the R_{Sh2} measurement.

C. 500 kV Generator based on OTS Diode

The capability of the OTS diode to generate high-voltage pulses is harnessed in this part of the study. Based on the preceding test bench, a 500 kV pulsed power Generator prototype, featuring an OTS Solid-State Opening Switch (GOSSOS) with a stored energy of up to 40 J, is proposed. In this generator, the OTS diode consists of four OTS-150 connected in series and the hole stack fits into a volume inferior to 2 liters.

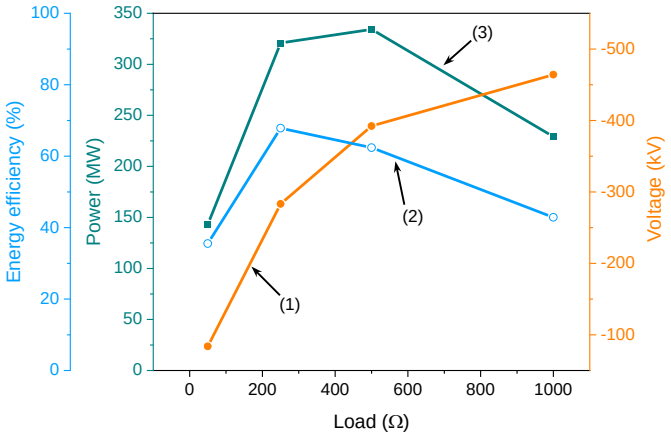

Fig. 9. Load characteristics of the GO-SSOS showing the load voltage V_{R_L} (1), the overall energy efficiency (2), and the load power (3), for different resistive loads ranging from 50 Ω to 1 kΩ (E_{C1} = 31.3 J).

Fig. 9 presents the load characteristic of the GO-SSOS at a resistive load varying from 50 Ω to 1 kΩ. Throughout this range, the stored energy remains fixed at 31.3 J. In this configuration, the system reaches a peak power of 335 MW, when the load was 500 Ω. The overall energy efficiency (E_{R_L}/E_{C1}) depending on the load is between 36% and 68%. It is important to note that the output energy only reflects the energy concentrated in the effective main pulse. In addition, the highest voltage of 465 kV is obtained at the load of about 1 kΩ.

The maximum generator output voltage amplitude of 515 kV is obtained in single pulse mode when the primary energy was increased to 39.2 J and the load fixed at 940 Ω. The rise time and FWHM of the pulse are 37 ns and 83 ns respectively.

The operation of the GO-SSOS at its maximum PRF of 60 Hz is presented in Fig. 10. A train of ten pulses with 500 kV amplitude at 60 Hz is shown in Fig. 10 (a). At this frequency, three sets of ten pulses are acquired in burst mode. The overlay of this burst is plotted in Fig. 10 (b) showing the excellent reproducibility of the pulses. The overall pulse-to-pulse amplitude and duration deviations are less than 2% and 10%, respectively.

It should be considered that two main components limit the PRF of the generator. The first is the capacitive charger, which requires about 15 ms to charge C1 to its maximum voltage of 28 kV. The second is the CX1174 thyratron, which, according to its datasheet, is capable of operating at a maximum PRF of 60 Hz when the current is 8 kA. Nevertheless, in the described experiment when the GO-SSOS operates at 60 Hz, the primary current is approximately 10 kA, which may reduce the thyratron lifetime.

The use of the GO-SSOS for a common pulsed power application, such as corona discharge, has been explored in this study. For this experiment, a high-voltage cable was connected to the output of the generator inside the oil tank. The other end of the cable was extended outside the oil, and terminated in a high-voltage electrode positioned approximately 15 cm from

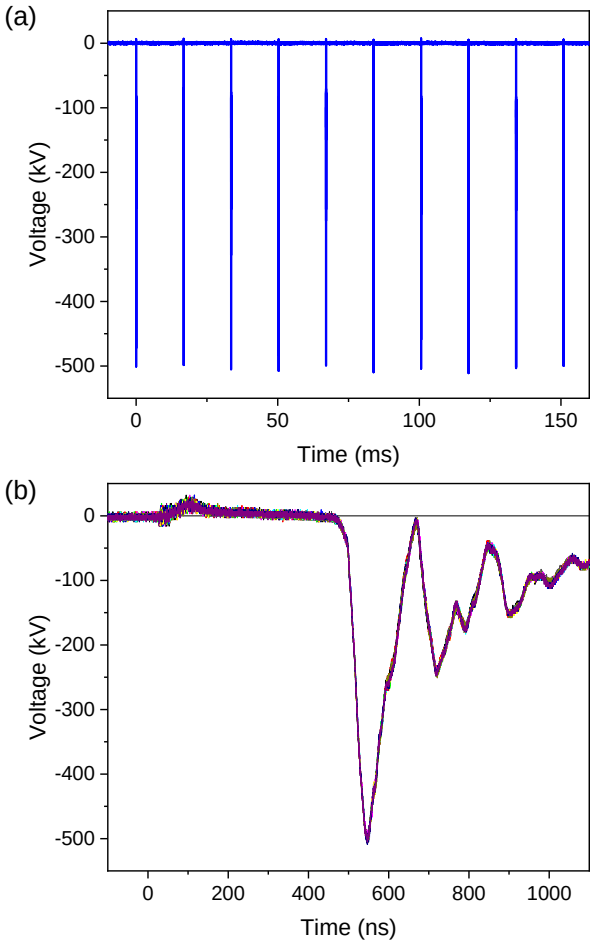

Fig. 10. Waveforms of the voltage across the load during operation of the GO-SSOS at 60 Hz (E_{C1} = 39.2 J, R_L = 940 Ω): (a) a train of 10 pulses, and (b) overlay of 30 pulses, acquired in the Peak Detection and Fast Frame modes of the oscilloscope.

a ground electrode. A needle-needle electrode configuration was adopted for this experiment. With a primary energy of 31.3 J and a pulse frequency of 50 Hz, the corona discharge generated within the 5-second burst is shown in Fig. 11. The experiments have successfully demonstrated the robustness of the generator control system against strong electromagnetic interference.

IV. Conclusion

This study introduces a nanosecond pulsed power generator based on an OTS solid-state opening switch for pulsed power applications. Despite the short reverse conduction time of the OTS diodes, their ability to produce high-voltage pulses was demonstrated. A voltage pulse having an amplitude of up to 515 kV with a rise time of 35 ns and an FWHM of 80 ns was obtained across a 1 kΩ load. In addition, the operation of the generator at a PRF of up to 60 Hz with high reproducibility of the pulses was shown. The PRF is limited by the primary thyratron switch and the high-voltage capacitor charger. Furthermore, an application of corona discharge was explored in the burst mode at a PRF of 50 Hz and a burst duration of 5 seconds. During testing, no degradation of

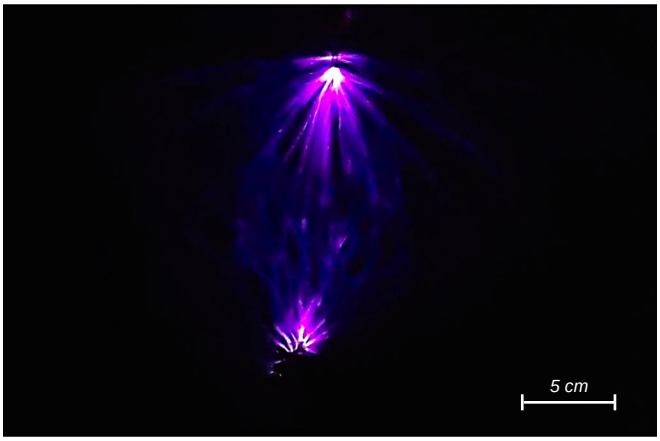

Fig. 11. Photo of corona discharge generated by the 500 kV GO-SSOS (E_{C1} = 31.3 J). The picture was taken using a regular mobile phone camera.

OTS diodes performance was observed after thousands of generated pulses. Thus, the reliability of the OTS-based pulsed power system has been confirmed. However, there is room for improvement in several parameters of this nanosecond high-voltage generator prototype, including volume reduction to achieve a more compact design and also the use of a solid-state primary switch to increase the frequency range. Pulse shaping and forming can also be considered. Further investigation of the OTS diode's current interruption mechanism is needed to get insights for future optimizations.

ACKNOWLEDGMENTS

We would like to express our gratitude to Sergei Rukin from the Institute of Electrophysics, Michael Barnes and Thomas Kramer from CERN, and Olaf Dressler from the Helmholtz-Zentrum Berlin for their generous help and contribution to this work. Their support and collaboration were invaluable to the success of our research.

REFERENCES

[1] M. Kristiansen, "Pulsed power applications," in *Ninth IEEE International Pulsed Power Conference*. IEEE, 1993, p. 6.

[2] K. Takaki, I. Yagi, S. Mukaigawa, T. Fujiwara, and T. Go, "Ozone synthesis using streamer discharge produced by nanoseconds pulse voltage under atmospheric pressure," *PPC2009 - 17th IEEE International Pulsed Power Conference*, no. December 2015, pp. 989–993, 2009.

[3] A. Gusev, S. Lyubutin, V. Patrakov, S. Rukin, B. Slovikovsky, M. Barnes, T. Kramer, and V. Senaj, "Fast High-Power Thyristors Triggered in Impact-Ionization Wave Mode," in *2019 IEEE Pulsed Power & Plasma Science (PPPS)*, vol. 2019-June. IEEE, jun 2019, pp. 1–4.

[4] S. Sokovnin and M. Balezin, "Surface irradiation installation for eggs based on URT-0,5M accelerator," *Radiation Physics and Chemistry*, vol. 196, no. January, p. 110137, jul 2022.

[5] R. A. Vazirov, S. Y. Sokovnin, A. S. Krivonogova, and A. G. Isaeva, "Radiation surface antimicrobial processing of poultry meat and by-products using the nanosecond low-energy electron beam," *Radiation Physics and Chemistry*, vol. 217, no. January, p. 111528, 2024.

[6] N. Ibrahimi, L. Vallet, F. M. Andre, L. Ariztia, M. Rivaletto, A. S. De Ferron, B. M. Novac, L. M. Mir, and L. Pécastaing, "A Subnanosecond Pulsed Electric Field System for Studying Cells Electropermeabilization," *IEEE Transactions on Plasma Science*, vol. 48, no. 12, pp. 4242–4249, 2020.

[7] C. Da Silva, C. Lamarche, C. Pichereaux, E. Mouton-Barbosa, G. Demol, S. Boisne, E. Dague, O. Burlet-Schiltz, F. Pillet, and M. P. Rols, "Bacterial eradication by a low-energy pulsed electron beam generator," *Bioelectrochemistry*, vol. 156, no. October 2023, 2024.

[8] Y. A. Kotov, G. A. Mesyats, S. N. Rukin, V. A. Telnov, B. G. Slovikovskii, S. P. Timoshenkov, and A. I. Bushlyakov, "Megavolt nanosecond 50 kW average power all solid state driver for commercial applications," *Digest of Technical Papers-IEEE International Pulsed Power Conference*, vol. 2, pp. 1227–1230, 1995.

[9] J. Gao, S. Li, B. Qian, J. Zhang, J. Zhang, and H. Yang, "Development of a GW-Level solid-state long pulse generator," *IEEE Transactions on Plasma Science*, vol. 47, no. 10, pp. 4512–4517, 2019.

[10] S. Li, J. Gao, C. Shi, X. Liu, and H. Yang, "Investigation on a fast rise time high voltage pulse transformer," *Review of Scientific Instruments*, vol. 90, no. 12, 2019.

[11] S. N. Rukin, "Pulsed power technology based on semiconductor opening switches: A review," *Review of Scientific Instruments*, vol. 91, no. 1, p. 011501, jan 2020.

[12] G. A. Mesyats, *Pulsed Power*. Boston, MA: Springer US, 2004.

[13] S. A. Darznek, S. N. Rukin, and S. N. Tsiranov, "Effect of structure doping profile on the current switching-off process in power semiconductor opening switches," *Technical Physics*, vol. 45, no. 4, pp. 436–442, 2000.

[14] S. N. Rukin, A. I. Gusev, S. Lyubutin, B. Slovikovsky, and S. Tsyranov, "OPERATION OF A SEMICONDUCTOR OPENING SWITCH AT ULTRAHIGH CURRENT DENSITY," no. 12, pp. 3–6, 2012.

[15] M. R. Degnon, A. I. Gusev, A. S. de Ferron, L. Pecastaing, G. Daulhac, A. Baranov, S. Boisne, and B. M. Novac, "Off-the-Shelf Diodes as High-Voltage Opening Switches," *IEEE Transactions on Plasma Science*, vol. 50, no. 10, pp. 3384–3392, oct 2022.

[16] A. I. Gusev, S. K. Lyubutin, S. N. Rukin, B. G. Slovikovsky, and S. N. Tsyranov, "High-current pulse switching by thyristors triggered in the impact-ionization wave mode," *Instruments and Experimental Techniques*, vol. 60, no. 4, pp. 545–550, 2017.

[17] J. Waldron, K. Brandmier, and V. Temple, "Ultra-fast, high reliability solid state thyratron, ignitron and thyristor replacement," *Digest of Technical Papers-IEEE International Pulsed Power Conference*, vol. 2015-Octob, pp. 676–680, 2015.

[18] M. R. Degnon, A. I. Gusev, A. S. de Ferron, L. Pecastaing, A. Baranov, C. Mielot, S. Boisne, M. J. Barnes, V. Senaj, T. Kramer, and B. M. Novac, "A Saturable Pulse Transformer Based on Nanocrystalline Magnetic Cores for an Adjustable Nanosecond High-Voltage Generator," *IEEE Transactions on Plasma Science*, pp. 1–9, 2023.

[19] e2v Teledyne, "CX1174 Deuterium-Filled Ceramic Thyratron," pp. 1–5. [Online]. Available: https://www.teledyne-e2v.com/en-us/Solutions_/Documents/datasheets/Thyratron/cx1174.pdf

[20] North Star High Voltage, "Thyratron Driver Manual and Application Note," North Star High Voltage, Tech. Rep., 2008. [Online]. Available: https://www.highvoltageprobes.com/wp-content/uploads/2019/11/ThyrDriveManual082908.pdf

[21] J. Choi, "Introduction of the Magnetic Pulse Compressor (MPC) - Fundamental Review and Practical Application," *Journal of Electrical Engineering and Technology*, vol. 5, no. 3, pp. 484–492, sep 2010.

[22] R. Pecquois, L. Pecastaing, A. De Ferron, M. Rivaletto, P. Pignolet, B. M. Novac, I. R. Smith, and R. J. Adler, "Simple and compact capacitive voltage probe for measuring voltage impulses up to 0.5 MV," *Review of Scientific Instruments*, vol. 83, no. 3, 2012.

[23] J. Lutz, H. Schlangenotto, U. Scheuermann, and R. De Doncker, *Semiconductor Power Devices*. Berlin, Heidelberg: Springer Berlin Heidelberg, 2011.